



CHORUS

This is the accepted manuscript made available via CHORUS. The article has been published as:

Central Charge of Periodically Driven Critical Kitaev Chains

Daniel Yates, Yonah Lemonik, and Aditi Mitra

Phys. Rev. Lett. **121**, 076802 — Published 14 August 2018

DOI: [10.1103/PhysRevLett.121.076802](https://doi.org/10.1103/PhysRevLett.121.076802)

Central charge of periodically driven critical Kitaev chains

Daniel Yates, Yonah Lemonik, and Aditi Mitra
*Center for Quantum Phenomena, Department of Physics,
 New York University, New York, NY, 10003, USA*
 (Dated: July 24, 2018)

Periodically driven Kitaev chains show a rich phase diagram as the amplitude and frequency of the drive is varied, with topological phase transitions separating regions with different number of Majorana zero and π modes. We explore whether the critical point separating different phases of the periodically driven chain may be characterized by a universal central charge. We affirmatively answer this question by studying the entanglement entropy (EE) numerically, and analytically for the lowest entangled many particle eigenstate at arbitrary non-stroboscopic and stroboscopic times. We find that the EE at the critical point scales logarithmically with a time-independent central charge, and that the Floquet micro-motion gives only sub-leading corrections to the EE. This result also generalizes to multi-critical points where the EE is found to have a central charge which is the sum of the central charges of the intersecting critical lines.

Periodic or Floquet driving has opened up new avenues of engineering correlated quantum systems with behavior qualitatively different from static systems [1, 2]. As in equilibrium, we wish to have universal descriptions of driven systems that do not depend on microscopic details. In equilibrium, critical states of matter possess a scale-invariance that leads to such universal descriptions. In one dimension (1D) static systems, this critical behavior can be captured by conformal field theories (CFTs) [3, 4]. Do such universal descriptions exist for 1D Floquet systems?

To address this question, we study a 1D Floquet system, the periodically driven Kitaev chain with nearest neighbor (nn) and next nearest neighbor (nnn) couplings [5–7]. The static Kitaev chain has a Z_2 invariant, which is enlarged to a Z invariant with time reversal symmetry (TRS). With driving, the system shows a rich phase diagram as the amplitude and frequency of the drive is varied, with topological phase transitions separating regions with different number of Majorana modes [8]. Moreover, the topological phases of the Floquet system is enhanced to $Z \times Z$ [9–13].

A universal characteristic of CFTs is their entanglement entropy (EE) [4]. Further, entanglement spectra (ES) (i.e, eigenvalues of the reduced density matrix) show an analogue of the bulk-boundary correspondence of topological systems [14, 15], and are also sensitive to criticality [16, 17]. In this paper we explore the EE and ES of driven Floquet states. These quantities have the advantage that unlike thermodynamic quantities, the EE [18] and ES extend naturally to non-equilibrium and driven systems, indeed to any quantum state. However, there are several subtleties in thinking about the ES in the Floquet setting. The ES is a set of levels that span a range determined by occupation probability of states, and thus has essentially the same appearance as the energy spectrum of a static Hamiltonian. However, in Floquet systems, energy is not conserved up to integer multiples of the drive frequency, so that the conserved quasi-

energy is periodic. Thus while there is one kind of zero-mode in a static Hamiltonian and in the corresponding ES, there are *two* kinds of such modes in a Floquet system: 0 and π modes. Since the ES is not periodic, there is no clear analog of the π -mode in the ES [8, 19].

A further wrinkle is that the $Z \times Z$ topological invariant and the quasi-energy spectrum are properties of the full drive cycle, while the ES and EE are constructed from the instantaneous quantum state. They are therefore sensitive to which point in the drive cycle they are calculated. Thus there is a conflict - one would expect that the ES and EE would carry information about the topological invariants, however they are sensitive to within-cycle dynamics (also known as Floquet micro-motion) which are not universal.

Thus it is unclear whether the critical points separating different Floquet phases have any universal, time-independent description in terms of the EE, as static critical points do. In this paper we find that the Floquet critical points *do* have a universal form for the EE, despite the micro-motion. In fact they have precisely the same scaling law $S \sim \frac{c}{3} \log L$ as the static system, where c is time-independent, and depends on the number of 0 and π modes. We also find equivalent behavior at multi-critical points separating more than two phases [20].

We study the Kitaev chain with nn (t_h, Δ) and nnn (t'_h, Δ') tunneling and pairing interactions. In terms of the complex fermion c_i and its Fourier transform c_k the Hamiltonian is,

$$\begin{aligned}
 H &= \sum_i \left[-t_h c_i^\dagger c_{i+1} - \Delta(t) c_i^\dagger c_{i+1}^\dagger - \mu(t) \left(c_i^\dagger c_i - \frac{1}{2} \right) \right. \\
 &\quad \left. - t'_h c_i^\dagger c_{i+2} - \Delta'(t) c_i^\dagger c_{i+2}^\dagger + h.c. \right] \\
 &= \sum_k (c_k^\dagger \ c_{-k}) H_{\text{BdG}}(k, t) \begin{pmatrix} c_k \\ c_{-k}^\dagger \end{pmatrix}. \tag{1}
 \end{aligned}$$

The periodic driving may be applied to the chemical potential (μ) or one or both of the pairing amplitudes

(Δ, Δ') . The results do not depend on which parameter is varying in time.

In momentum space, the Hamiltonian is $H_{\text{BdG}}(k, t) = -\vec{d}(k, t) \cdot \vec{\sigma}$, where $d_x(k, t) = 0$, $d_y(k, t) = \Delta(t) \sin(k) + \Delta'(t) \sin(2k)$, $d_z(k, t) = t_h \cos(k) + t'_h \cos(2k) + \mu(t)/2$. For the numerical demonstrations, we drive both Δ and Δ' , keeping μ static. In units of $t_h = 1$, the parameters used are, $\Delta(t) = \Delta + 4 \sin(\Omega t)$, $\Delta'(t) = \Delta' + 4 \sin(\Omega t)$, $t'_h = -2$, $\Delta = 1$, $\Delta' = -2$, $\Omega = 12$.

The static Hamiltonian falls in the BDI classification [21] with an integer Z characterizing the number of Majorana zero modes. This also equals the number of times the spinor $\vec{d}(k)/|\vec{d}(k)|$ winds in the y - z plane in momentum space. Fig. 1 describes the static system. As μ is tuned, the system shows several topological phases. These phases are distinguished by the number of Majorana zero modes in the energy spectrum (top panel) and the ES (middle panel). In addition the critical points separating the topological phases are characterized by an EE that scales as (bottom panel) $S = (c/3) \log L$, where L is the size of the sub-system associated with the reduced density matrix, and c is the central charge. For a critical point separating a phase with Z Majorana modes from one with Z' Majorana modes, the numerically extracted central charge is $c = |Z - Z'|/2$ [22]. In this paper we wish to understand how this fundamental result for the scaling of the EE of critical static phases, generalizes to critical Floquet phases.

In particular we are interested in the entanglement scaling of the Floquet ground state (FGS) which is a half-filled many-body eigenstate of the Floquet Hamiltonian $H_F = H(t) - i\partial_t$. This eigenstate is a Slater determinant of the time periodic Floquet modes $|\phi(k, t)\rangle$, defined as the eigenmodes of H_F , $H_F|\phi(k, t)\rangle = \epsilon_k|\phi(k, t)\rangle$. ϵ_k are the quasi-energies, and are restricted within a Floquet Brillouin zone (FBZ) of size Ω [23, 24]. The half-filled state corresponding to the FGS is such as to ensure area law scaling of the EE when the system has a gap in the quasi-energy spectrum. Concretely, restricting the quasi-energy spectrum to lie between $-\Omega/2, \Omega/2$, and noting that chiral symmetry of the Floquet Hamiltonian causes the quasi-energy spectra to come in pairs of $\pm|\epsilon_k|$, the FGS corresponds to occupying with probability 1 all Floquet modes with say negative quasi-energy. This should be contrasted with a half-filled state obtained from unitary time-evolution under $H(t)$ from an arbitrary initial state, where such a state will show volume law scaling of the EE at steady-state [8, 19].

We briefly explain how the ES and EE are studied numerically and analytically. The underlying principle is that for a system of free fermions, the eigenvalues of the reduced density matrix can be extracted from the eigenvalues of only the two-point correlation function, a consequence of Wick's theorem [25, 26]. The relevant

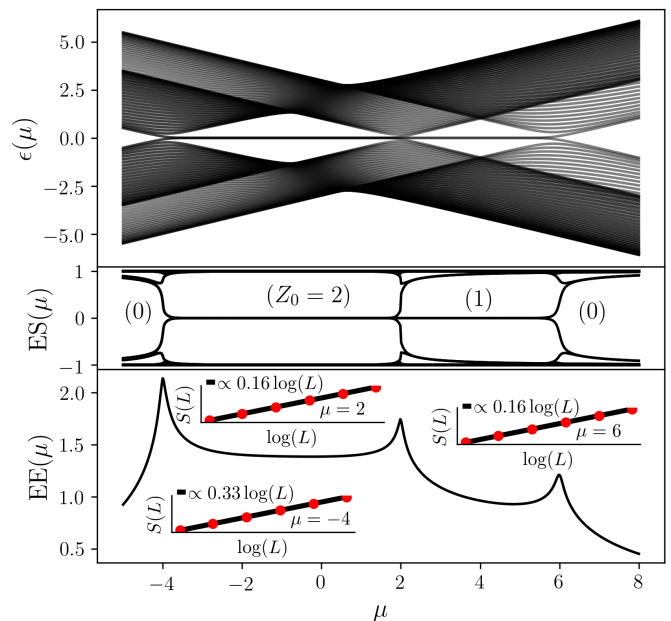


FIG. 1: Static system, all plotted against μ . Top panel, the energy levels of a wire with length $L = 75$. Middle panel, the ES for an entanglement cut of length $L = 75$ with periodic boundary conditions applied to the full density matrix. Bottom panel, the EE of the same. The insets in the bottom panel show how the EE (or S) at the critical points scale with L with $400 \leq L \leq 600$.

correlation matrix for our half-filled state is

$$G_{i,j}(t) = \int_{-\pi}^{\pi} \frac{dk}{2\pi} e^{ik(i-j)} \mathcal{M}_k(t), \quad (2)$$

where i, j index the physical sites within the entanglement cut, \mathcal{M} is a 2×2 matrix which for the static ground state and FGS are respectively,

$$\mathcal{M}_{k,\text{static}} = \frac{\vec{d}(k) \cdot \vec{\sigma}}{|\vec{d}(k)|}; \mathcal{M}_{k,\text{FGS}}(t) = \langle \phi(k, t) | \vec{\sigma} | \phi(k, t) \rangle \cdot \vec{\sigma}. \quad (3)$$

G_{ij} is a hermitian matrix whose expansion in terms of Pauli matrices implies that eigenvalues come in pairs $\pm\lambda_i$, giving an EE,

$$S = -\frac{1}{2} \sum_{\alpha=\pm, \lambda_i} \left[\left(\frac{1 - \alpha\lambda_i}{2} \right) \ln \left(\frac{1 - \alpha\lambda_i}{2} \right) \right]. \quad (4)$$

The Majorana modes in the ES are pinned exactly at zero entanglement energies (middle panel, Fig. 1).

There are some key differences between static and Floquet topological phases. In the presence of Floquet driving, the definition of TRS is subtle. There are two TRS points t^* within a cycle where the Hamiltonian obeys $H(t + t^*) = H(-t + t^*)$ for all t . For our drive, these are $t^* = \pi/2\Omega, 3\pi/2\Omega$.

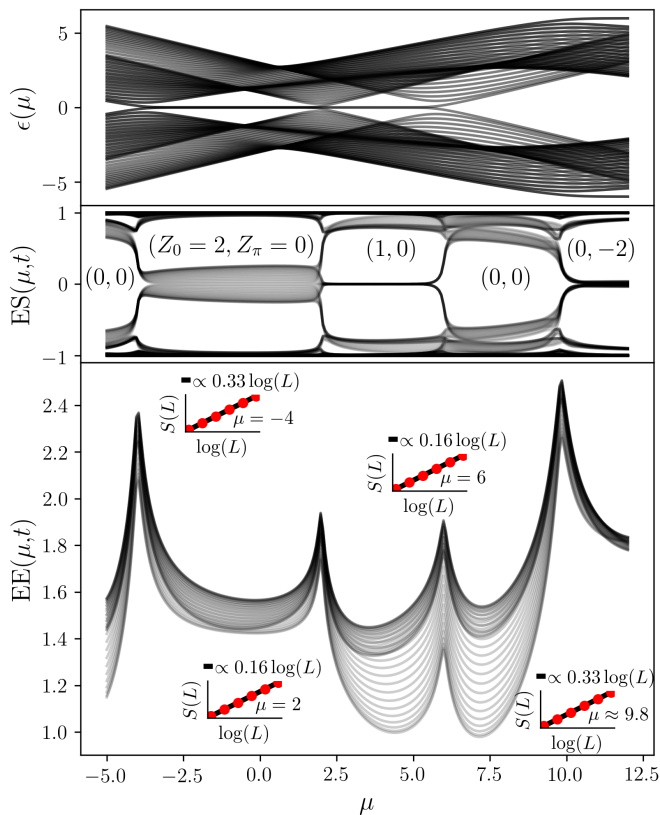


FIG. 2: Floquet system, all plotted against μ . Top panel, the quasi-energy levels of the wire with size $L = 50$. The π modes are visible at the FBZ boundary $|\epsilon| = \Omega/2 = 6$ for $\mu > 10$. Middle panel, the ES at several different times within a period (different solid lines) for an entanglement cut of size $L = 50$. Strongest time-dependence are at zero entanglement energies. Bottom panel, the corresponding time dependent EE (solid lines are for different times within a period). The insets in the bottom panel show how the EE (or S) at the critical points scale with L with $400 \leq L \leq 600$. The leading logarithmic contribution at the critical points is time-invariant.

The quasi-energy spectrum hosts Majorana modes that are either pinned at zero quasi-energy, or at the Floquet zone boundaries. We will denote the former as Majorana zero modes (MZM), and the latter by Majorana π modes (MPM). The Floquet phase is now characterized by $Z_0 \times Z_\pi$ where $Z_0 (Z_\pi)$ refers to the number of MZMs (MPMs). Fig. 2 (top panel) displays the quasi-energy levels for the time periodic chain. As μ is increased, several transitions are visible, going from trivial to 2MZM to 1MZM to trivial to 2MPM.

Since quasi-energies are not sensitive to the micro-motion, while EE and ES are, this leads to some ambiguity between the topological characterization via the quasi-energy, and that from the entanglement. The topo-

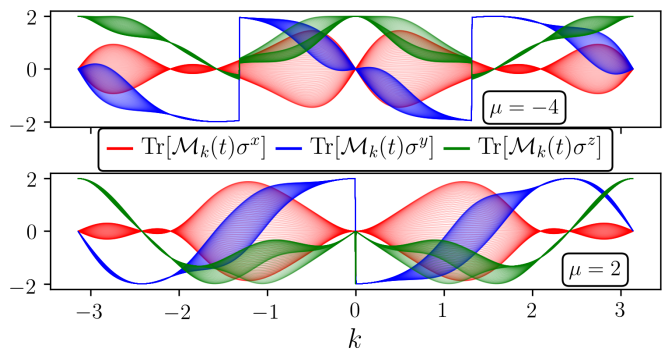


FIG. 3: Discontinuities in $\mathcal{M}_k(t)$ for the FGS, for several times during a driving period (different solid lines) and at two different critical μ . The discontinuities send the Bloch-vector to the opposite side of the sphere at all times, with the orientation of the jump varying in time. Number of discontinuous eigenvalues of \mathcal{M}_k are $N_T = 4$ (top) and $N_T = 2$ (bottom). The discontinuities in the σ_x projection are difficult to see. Away from the critical μ values (not shown), all the projections are continuous.

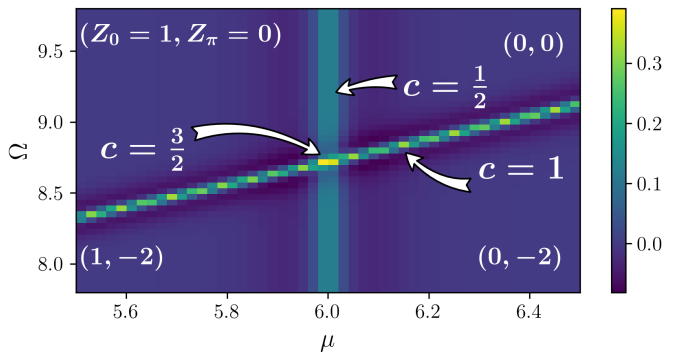


FIG. 4: Phase diagram of the prefactor to $\log(L)$ in the EE scaling for the FGS, as a function of μ and Ω . The multi-critical point separates the four phases $(Z_0, Z_\pi) = (0, 0), (1, 0), (1, -2), (0, -2)$. The leading logarithmic scaling at the critical lines and multi-critical point are time independent.

logical phase transitions are visible in the ES (middle panel) in a different way. Firstly the ES is characterized by a single gap, and all edge modes have to lie in this gap. In addition, the winding of the Floquet states in momentum space is strictly speaking well-defined only at the two TRS times. At other times of the drive, the Floquet modes acquire a non-zero projection along all three directions $\hat{x}, \hat{y}, \hat{z}$ so that the winding is ill-defined. This leads to an ES where the Majorana zero (entanglement) energy modes appear only at the two discrete times t^* in the ES, while at other times the Majorana modes on the same sides of the entanglement cut couple

to each other forming complex fermions. Although these complex fermions are still localized at the entanglement cuts, their entanglement energies are no longer pinned at zero. Thus while at the two TRS times, the number of Majorana modes in the ES are $|Z_0 \pm Z_\pi|$ respectively [27], at other times, the ES shows a Z_2 invariance. The reason for Z_2 is that if there are an odd number of Majorana modes at an entanglement cut, one unpaired Majorana mode persists when $t \neq t^*$. This physics is highlighted in Fig. 2 (middle-panel) where the ES through a series of topological phases obtained from varying μ are shown at several different times of the drive cycle. The time-dependence is the strongest at zero entanglement energies [27], with the zero modes appearing only at special times t^* .

What is remarkable is that the EE (bottom panel Fig. 2) constructed out of this ES, despite the fact that the zero modes exist at only two discrete times during a cycle, still scales logarithmically at the critical points with a time independent central charge. Note that at all points including the critical points, the EE is time dependent. This makes the time-independent central charge non-trivial. The time-dependence from micro-motion only gives sub-leading corrections, in size of the entanglement cut L , to the EE at the critical point. In contrast, away from the critical points, due to the presence of the gap, area law holds. In this case, the micro-motion affects the EE to leading order. This is apparent in the bottom panel of Fig. 2 where the time-dependence of the EE is largest away from the critical points.

Ref. [27] shows how the EE scales as one crosses the several topological phases as a function of time and system-size. Irrespective of the micro-motion, the entanglement scales as in a static critical phase, but with a modified central charge,

$$c = \left(|Z_0 - Z'_0| + |Z_\pi - Z'_\pi| \right) / 2, \quad (5)$$

with any deviations from the above decreasing with momentum space resolution.

We explain this robust central charge as follows. The logarithmic scaling originates from a discontinuity in the matrix \mathcal{M}_k . For example, for non-interacting complex fermions ($\Delta = \Delta' = 0$), \mathcal{M}_k is a scalar with a step-function at the Fermi momentum. This leads to a power-law $G_{ij} \sim 1/|i - j|$ in the correlation function, and an EE that scales with $(1/3) \ln L$, and hence $c = 1$ [28, 29]. For the BdG Hamiltonians under consideration here, the discontinuity is reflected in special k points where the dispersion $\epsilon(k^*) = 0$, and $\mathcal{M}(k^{*+}) \neq \mathcal{M}(k^{*-})$ [30]. For example, for $\Delta' = 0, t'_h = 0, t_h = \Delta, \mu = 2t_h$, $\mathcal{M}_k = \frac{\cos(k/2)}{|\cos(k/2)|} [\cos(k/2)\sigma_z + \sin(k/2)\sigma_y]$. The dispersion vanishes at $k^* = \pi$, and around this point \mathcal{M}_k has the discontinuity $\mathcal{M}(\pi^+) = \sigma_y, \mathcal{M}(\pi^-) = -\sigma_y$. This discontinuity gives rise to power-law correlations in position,

and a corresponding EE which scales as $S = (c/3) \ln L$ with $c = 1/2$ [27].

Consider another example with mnm terms that can give rise to multiple Majorana modes. For $\Delta = \Delta' = t_h = t'_h, \mu = 2t_h$, $\mathcal{M}_k = \frac{1+2\cos(k)}{|1+2\cos(k)|} [\cos(k)\sigma_z + \sin(k)\sigma_y]$. The dispersion now vanishes at two points in momentum space corresponding to $k^* = \pm 2\pi/3$. Across these k^* , the \mathcal{M}_k are discontinuous as follows, $\mathcal{M}(k^{*+}) = \sigma_y = -\mathcal{M}(k^{*-})$. Each of these points gives a central charge of $1/2$, implying a total central charge of $c = 1$. Thus quite simply, the total central charge is $c = N_T/4$ where N_T is the number of discontinuous eigenvalues of \mathcal{M}_k . Ref. [27] demonstrates these discontinuities at the critical points of the static system shown in Fig. 1.

Similar to the static case, the central charge of the Floquet system follows from the nature of the discontinuities in the $\mathcal{M}_{k,\text{FGS}}$. Fig. 3 (and Ref. [27]) shows that despite the micro-motion of the Floquet states, $\mathcal{M}_{k,\text{FGS}}$ maintains a time-independent jump across momenta k^* at which the quasi-energy vanishes. This fact holds for both changes in Z_0 and/or Z_π at the transition. The origin of the discontinuity is that the FGS is constructed from ‘‘filling’’ all quasi-energy levels of the same band, introducing a ‘‘Fermi’’ point in momentum space. This discontinuity can again be indexed by the number of discontinuous eigenvalues N_T . Fig. 3 plots $\mathcal{M}_{k,\text{FGS}}$ projected onto the Pauli matrices for many times during the drive cycle, and for several different Floquet critical points. We find that $N_T = 2(|Z_0 - Z'_0| + |Z_\pi - Z'_\pi|)$. The time-dependence only changes the location of the jump on the Bloch sphere. While clearly the leading scaling of the EE is like that of a static critical theory with a well defined central-charge, yet the EE does show periodicity in time. This periodic behavior only affects the sub-leading behavior in the EE at the critical point.

We now give analytic arguments for the numerical results. Expanding around $k = k^*$ where the dispersion vanishes, and therefore \mathcal{M}_k is singular, we write,

$$\mathcal{M}_{k,\text{FGS}} \simeq \frac{(k - k^*)}{|k - k^*|} \sigma_1(t) + \vec{g}_k(t) \cdot \vec{\sigma}, \quad (6)$$

where $\sigma_1(t) = \hat{n}(t) \cdot \vec{\sigma}$ with \hat{n} a unit vector. The discontinuous prefactor contains the physics of the ‘‘Fermi’’-point associated with the FGS. In contrast \vec{g}_k is a smooth function of k . The time-dependence of \vec{g}_k, σ_1 are due to Floquet micro-motion. In the static problems [31], $\sigma_1 = \sigma_y$. Regardless of the value of $\sigma_1(t)$, as one crosses k^* , the matrix jumps from σ_1 to $-\sigma_1$, and $N_T = 2$ at all times. Eq. (6) is valid whether we have jumps in Z_0 and/or Z_π , where the difference between the two kinds of modes is encoded in the micro-motion i.e, the precise time-dependence of $\sigma_1(t), g(t)$.

The Fourier transform of Eq. (6) is

$$G_{ij}(t) \sim i \frac{e^{ik^*(i-j)}}{\pi(i-j)} \sigma_1(t) + \vec{g}_{k=0}(t) \cdot \vec{\sigma} \delta(i-j) + \vec{g}'_{k=0}(t) \cdot \vec{\sigma} \delta'(i-j) + \dots \quad (7)$$

Thus the smooth function \vec{g}_k gives only short ranged correlations. The discontinuity at $k = k^*$, despite the oscillation $e^{ik^*(i-j)}$ gives [27] logarithmic scaling of the EE. When there are many ‘‘Fermi’’ points, the EE from each singular point combines additively. Note that one cannot rule out non-topological gap closings, in which case Eq. (5) provides a lower bound.

Floquet micro-motion only affects short distance correlations because the micro-motion is over a time $t \leq \Omega^{-1}$, and is therefore associated with a finite spatial range t_h/Ω in units of the lattice spacing. This short distance physics cannot affect the power-law tail of Eq. (7) which extends over arbitrary long distances. However when the system is gapped, and the correlations are short-ranged, then the micro-motion is the leading correction, giving a strong time-dependence to the EE (Fig. 2).

The richness of phases under periodic drive leads not only to critical points separating two different phases, but also multi-critical points. Fig. 4 shows a multi-critical point separating four phases. This multi-critical point is the meeting point of two critical lines, and is associated with a central charge $c = c_1 + c_2$, where $c_{1,2}$ are the central charges of the two intersecting critical lines. For the example shown, $c = 3/2 = 1 + 1/2$.

We have shown that a critical (multi-critical) point separating two (or more) Floquet phases, despite the time-dependence has a universal behavior for the EE, namely that it scales as $(c/3) \ln L$ where the central charge accounts for MZMs and MPMs (Eq. (5)). The time-dependence due to micro-motion gives sub-leading corrections that obey the area law. Away from the critical point, these sub-leading corrections become the dominant correction, and the EE shows a strong time-dependence. How these results are affected by interactions is an interesting open question.

Acknowledgements: This work was supported by the US Department of Energy, Office of Science, Basic Energy Sciences, under Award No. DE-SC0010821.

-
- [1] T. Oka and S. Kitamura, arXiv:1804.03212 (unpublished).
 - [2] J. Cayssol, B. Dóra, F. Simon, and R. Moessner, Phys. Status Solidi RRL **7**, 101 (2013).
 - [3] G. Vidal, J. I. Latorre, E. Rico, and A. Kitaev, Phys. Rev. Lett. **90**, 227902 (2003).
 - [4] P. Calabrese and J. Cardy, Journal of Statistical Mechanics: Theory and Experiment **2004**, P06002 (2004).
 - [5] A. Y. Kitaev, Physics-Uspekhi **44**, 131 (2001).
 - [6] Y. Niu, S. B. Chung, C.-H. Hsu, I. Mandal, S. Raghu, and S. Chakravarty, Phys. Rev. B **85**, 035110 (2012).
 - [7] M. Thakurathi, A. A. Patel, D. Sen, and A. Dutta, Phys. Rev. B **88**, 155133 (2013).
 - [8] D. J. Yates and A. Mitra, Phys. Rev. B **96**, 115108 (2017).
 - [9] T. Kitagawa, E. Berg, M. Rudner, and E. Demler, Phys. Rev. B **82**, 235114 (2010).
 - [10] M. S. Rudner, N. H. Lindner, E. Berg, and M. Levin, Phys. Rev. X **3**, 031005 (2013).
 - [11] J. K. Asbóth, B. Tarasinski, and P. Delplace, Phys. Rev. B **90**, 125143 (2014).
 - [12] J. K. Asbóth and H. Obuse, Phys. Rev. B **88**, 121406 (2013).
 - [13] R. Roy and F. Harper, Phys. Rev. B **96**, 155118 (2017).
 - [14] M. Levin and X.-G. Wen, Phys. Rev. Lett. **96**, 110405 (2006).
 - [15] A. Kitaev and J. Preskill, Phys. Rev. Lett. **96**, 110404 (2006).
 - [16] H. Casini and M. Huerta, Journal of Physics A: Mathematical and Theoretical **42**, 504007 (2009).
 - [17] Y. Lemonik and A. Mitra, Phys. Rev. B **94**, 024306 (2016).
 - [18] A. Russomanno and E. G. D. Torre, EPL (Europhysics Letters) **115**, 30006 (2016).
 - [19] D. J. Yates, Y. Lemonik, and A. Mitra, Phys. Rev. B **94**, 205422 (2016).
 - [20] W. Berdanier, M. Kolodrubetz, S. Parameswaran, and R. Vasseur, arxiv:1803.00019 (2018).
 - [21] S. Ryu, A. P. Schnyder, A. Furusaki, and A. W. W. Ludwig, New Journal of Physics **12**, 065010 (2010).
 - [22] R. Verresen, R. Moessner, and F. Pollmann, Phys. Rev. B **96**, 165124 (2017).
 - [23] J. H. Shirley, Phys. Rev. **138**, B979 (1965).
 - [24] H. Sambe, Phys. Rev. A **7**, 2203 (1973).
 - [25] I. Peschel and V. Eisler, Journal of Physics A: Mathematical and Theoretical **42**, 504003 (2009).
 - [26] L. Amico, R. Fazio, A. Osterloh, and V. Vedral, Rev. Mod. Phys. **80**, 517 (2008).
 - [27] See Supplemental Material.
 - [28] M. M. Wolf, Phys. Rev. Lett. **96**, 010404 (2006).
 - [29] D. Gioev and I. Klich, Phys. Rev. Lett. **96**, 100503 (2006).
 - [30] F. Ares, J. G. Esteve, F. Falseto, and A. R. de Queiroz, Phys. Rev. A **92**, 042334 (2015).
 - [31] I. Peschel, Journal of Statistical Mechanics: Theory and Experiment **2004**, P06004 (2004).